

LOWER LIMIT FOR THE MASS OF THE INTERMEDIATE BOSON

J.M. Gaillard and B. Hahn, CERN.

(presented by B. Hahn).

I. INTRODUCTION

In high-energy neutrino experiments the intermediate boson would be produced mainly through the reaction¹⁻³⁾:

$$\nu + p \rightarrow p + W^+ + \mu^- , \quad (1)$$

provided its mass is not too high. It would then decay within 10^{-18} seconds through various channels:

$$W^+ \rightarrow \mu^+ + \nu \quad (2)$$

$$W^+ \rightarrow e^+ + \nu \quad (3)$$

$$W^+ \rightarrow \text{mesons} . \quad (4)$$

The rates for (2) and (3) are practically equal (universality); the branching ratio $B = (W \rightarrow l + \nu / W \text{ total})$ is not well known.

Among the events produced during the CERN neutrino experiment in the bubble chamber and in the spark chamber, a search has been made for boson production and its subsequent decays^{4,5)}. For the determination of the rates it was assumed that the neutrino spectrum follows Van der Meer's computations⁶⁾ and that the cross-sections and the kinematics for boson production and decay are those given in Ref. 3. No evidence has been found for the boson, and different lower limits for its mass have been derived under various assumptions.

Decay mode	B	M_W (GeV/c ²)	Confidence level ^{*)}	Reference
$W^+ \rightarrow \text{mesons}$	0	> 1.5	77%	(4)
$W^+ \rightarrow e^+ + \nu$	100%	> 1.8	80%	(4)
$W^+ \rightarrow e^+ + \nu$	50%	> 1.8	85%	(5)
$W^+ \rightarrow \mu^+ + \nu$	50%	> 1.8	98%	(5)

Cross-sections have now been computed by Wu et al.⁷⁾ for boson masses up to 2.5 GeV/c². They include W production on neutrons due to the neutron magnetic moment; this contribution amounts to about 20% of the total cross-section and was not taken into account in the previous computations.

*) These confidence levels have been computed by the authors of the present paper on the basis of the data as they have been published.

In the present paper combined results of a more extensive study of the spark chamber and the bubble chamber data are presented. A lower limit is given for the boson mass with the branching ratio B as a free parameter.

II. EXPERIMENTAL SET-UP

The spark-chamber apparatus has already been described in some detail^{5,8)}. In view of the analysis which is reported in this article, we shall give some relevant data on the set-up. Figure 1 shows the detailed structure of the magnetized iron region. The magnetic field inside the 5 cm iron plates is 18 kG. Three pictures are taken for each event, two from the side and one from the top, providing 90° stereo. Most of the analysis presented in this paper is based on a study of the events originating in the fiducial volume, drawn in Fig. 1 (15 tons of iron). This magnetized iron region is followed by a non-magnetized region of similar structure. Two stereo views only are available in that section. The set-up ends with a thick-plate region (5- 15 cm of lead) which is followed by two 15 cm magnetized iron slabs. Events originating in that region have been used for part of the analysis.

The details of the bubble chamber are given in Ref. 4.

III. NEUTRINO SPECTRUM AND BOSON PRODUCTION

Van der Meer has computed the neutrino spectrum at the spark-chamber position⁶⁾ using the pion and kaon production spectra. This computed spectrum is shown in Fig. 2. As the elastic cross-section for low four-momentum transfer [$q^2 \leq 0.2 \text{ (GeV/c)}^2$] does not depend much on the form factors, one can, in principle, deduce experimentally the neutrino spectrum from these low q^2 events⁹⁾. A first attempt⁵⁾ in that direction gave two-and-a-half times more events than were expected from the Van der Meer spectrum in the energy region above 4 GeV.

The main difficulty in this spectrum determination arises from the contamination due to inelastic events which look like elastic events. This background comes almost exclusively from the inelastic events in which a single low-energy pion is produced and is either reabsorbed in the nucleus or not recognized in the spark chamber. For low q^2 values, low-energy pions are produced predominantly from the decay of the $(\frac{3}{2}, \frac{3}{2})$ resonance. The cross-section for N^* production has been computed by Berman and Veltman¹⁰⁾ and its value, for low q^2 , which is practically independent of the form factors involved, is twice the elastic cross-section. Assuming that all the low q^2 isobar events are mistaken for elastic events, the experimental spectrum is approximately reduced to the Van der Meer spectrum. With a more conservative estimate of the background, the Van der Meer spectrum can be considered as a lower limit for the neutrino flux and will be used in what follows.

From that spectrum and from the cross-sections of Wu et al.⁷⁾, the rate of the boson production has been calculated as a function of the neutrino energy and is shown in Fig. 3. Since the production cross-sections have been computed only up to 10 GeV, they have been extrapolated to 15 GeV.

IV. MUONIC DECAY

The production of a boson and its subsequent muonic decay would be observed as a pair of muons: a negative muon associated with the boson [reaction (1)], and a positive muon resulting from its decay [reaction (2)]. These events would appear in the magnetized iron set-up as a pair of non-interacting particles of opposite charge. A search has been made in the magnetized iron set-up for such events.

1. Selection of events

Only events which occur in the first 15 tons of the magnetized iron section are accepted for inspection. For this fiducial region it is possible to determine the sign of muons in 95% of the cases, provided they do not escape before having traversed six iron plates. To be selected, an event must fulfil the following conditions:

i) It contains at least two tracks both of which have visible range larger than 30 cm of iron when projected along the neutrino direction. This cut in range corresponds to a minimum momentum of 470 MeV/c for a muon.

ii) The two tracks do not interact. An interaction is defined as: a single scattering with an angle $\geq 12^\circ$ in any stereo view, after which the track continues through at least three chambers (≥ 15 cm of iron); or as a star with two or more prongs, where a prong is defined by aligned sparks over at least three chambers.

iii) The sign combination of the two particles is: (+,-), (+,?), (-,?) or (?,?). Tracks for which the sign cannot be determined, because they show too small sagitta, are mostly due to protons which stop or to very energetic particles which escape from the chamber.

In some cases a single scattering, while not falling into the interaction definition, can modify the magnitude and even the sign of the curvature.

Table 1 gives a list of the events which fulfilled the selection criteria. In addition we have found two (+,+) events and eight (-,-) events which have been rejected in view of criterium (iii).

Figure 4 shows the sagitta versus range distribution for the stopping particles which are in the sample. The sagitta distribution of stopping μ^- have been determined experimentally. In the diagram of Fig. 4, 95% of the stopping muons will fall in the region above the solid line. If all stopping particles in our sample were muons, not more than two events should lie below the solid line; instead there are 19 events. These tracks are due mainly to stopping protons which have a sagitta about four times smaller than that of a muon of the same range. The 19 events which fall below the solid line of Fig. 4 have been eliminated from the sample. Taking into account the number of events without a stopping particle, this new selection criterium eliminates only 3% of the boson events which could be contained in the sample.

When these various criteria have been applied 33 events are left to be compared with about 5,000 neutrino events produced in the same volume. Figure 5 shows one of the events.

2. Range distribution of pairs

Figure 6 presents a two-dimensional plot of the 33 events which constitute the final sample. Each point corresponds to one event; in abscissa and ordinate the ranges of the negative and of the positive tracks are given respectively. In all 33 events the sign of at least one of the two tracks is known; when the second track has a null sagitta, it is assumed that the two tracks have opposite signs.

In muon pairs due to an intermediate boson, the positive muon should have, on the average, a range about 1.5 times longer than the negative one. This property is practically independent of the neutrino spectrum. Figure 6 shows a completely different behaviour for the events, indicating that most of them cannot be due to boson production.

3. Range distribution of the positive tracks

In order to further investigate this problem, the integral range distribution of the positive tracks has been plotted in Fig. 7. For each range value the ordinate gives the number of positive tracks which have a visible length greater than that range. The theoretical curves drawn in Fig. 7 give the range distributions of the positive muons due to boson decays for various values of the boson mass. They have been computed by using the Van der Meer neutrino spectrum⁶⁾, the cross-sections of Wu et al.⁷⁾, and the boson production and decay kinematics from Bell and Veltman^{2,3)}, and are corrected for experimental losses due to escape of the tracks. The branching ratio $B = (W \rightarrow \ell^+ + \nu/W^+ \text{ total})$ is assumed to be 50%. This plot also shows clearly, from the difference in shape between the experimental and theoretical distributions, that the majority of the events are not due to boson production.

The question of the boson decay kinematics requires some further discussion. The μ^+ angular distribution and momentum spectrum have been evaluated under the assumption that in the production process the boson is completely polarized backward. Therefore, the positive muon is emitted backwards in the boson system. This property emerges from a detailed theoretical study of the production process. If it should turn out that the boson is not so strongly polarized, the angular distribution of the positive muons would be more peaked forward and its momentum would be higher. These two facts would lead to an even more pronounced difference between the theoretical and experimental range distributions of the positive tracks.

4. Expected and observed number of events

A comparison is made between the expected and observed number of events for various cuts on the positive and negative tracks. Figure 7 shows that to eliminate most of the background events, one has to apply cuts in range longer than the initial 30 cm one, at least for the positive tracks.

The results will be listed for three different cuts:

- 45 cm of iron on both tracks
- 55 cm of iron on both tracks
- 30 cm of iron for the negative track
and 70 cm for the positive one.

In addition to the analysis performed on the events produced in the magnetized iron region, the events originating in the thick-plate region have been studied in a similar way. This last section of the set-up ends with two thick slabs (15 cm) of magnetized iron which permit a determination of the particle signs. However, as the magnetized iron is at the end of the set-up, there is no possibility of making a sagitta versus range study; furthermore, no 90° stereo being available, the interactions are harder to detect. Because of these two drawbacks with respect to the magnetized iron region, a uniform cut of 60 cm on both tracks has been applied for the events originating in the thick-plate region.

In Table 2 the total number of expected and observed events in the two regions are given for different values of the boson mass with $B = 50\%$. In each of the three cases a contribution of about one event is expected from the decay in flight of a pion, which associated with the initial negative muon will give a muon pair.

V. NON-LEPTONIC DECAYS

The results given in the previous section have been derived under the assumption that 50% of the bosons decay through the leptonic modes. Generalizing to SU_3 the CVC and the PCAC hypotheses, Mani and Nearing¹¹⁾ have computed the rates of the two-meson decay modes of the intermediate boson. They predict that these decay modes should become increasingly dominant over the leptonic decays for higher boson masses. According to their computations the branching ratio $[W \rightarrow l + \nu / (W \rightarrow 2 \text{ mesons}) + (W \rightarrow l + \nu)]$ would be 50% for $M_W = 1.5 \text{ GeV}/c^2$, and 20% for $M_W = 2.5 \text{ GeV}/c^2$. Other non-leptonic modes of the boson should lead to even smaller values for the branching ratio B .

A search has been made by Block et al.⁴⁾ for possible non-leptonic decays of the boson in the CERN heavy liquid bubble chamber. From the total number of inelastic neutrino events, which have a visible energy larger than 6 GeV, a total meson charge + 1, and a meson invariant mass between 1 GeV/c² and 2 GeV/c², they have derived a lower limit $M_W = 1.5 \text{ GeV}/c^2$ under the assumption that $B = 0$.

In addition to the criteria which have been applied in the bubble chamber study, it should be noted that in boson production the average momenta of the μ^- and W^+ are approximately in the ratio of their masses. This is a kinematical feature practically independent of the theory used to compute the process; it leads to a low momentum peak in the momentum distribution of the negative muons associated with the production of a W^+ .

In view of this general property, we have searched for non-leptonic decays of the intermediate boson in the thin-plate aluminium region (5 mm plates)⁶⁾ of the spark chamber set-up. The total energy of the visible tracks can be estimated without difficulty in most of the inelastic events, provided only the events originating inside a central portion of the chamber are considered. Furthermore, for the high-energy events the negative muon reaches the magnetized iron region in most of the cases and is, therefore, identified. Its momentum is measured with an accuracy of about 30% from the curvature or 10% from the range when it stops inside the set-up.

All events produced in the thin-plate region which fulfilled the following conditions have been selected:

- i) The apex is within a fiducial volume whose boundaries lie 20 cm inside the limiting surfaces of the chamber.
- ii) The event contains: ≥ 4 tracks, $\geq (2 \text{ tracks} + n \text{ showers})$ ($n \geq 1$), or $\geq (2 \text{ tracks} + 1 \nu^0)$. These are the minimum configurations for a boson event.
- iii) The total estimated energy of the visible tracks and showers is > 3.5 GeV.

One hundred and thirty-one events fulfilled the first two criteria; for about 15 of them the use of the third criterium has presented some difficulties, because too many tracks escaped from the chamber and the energy directly visible was less than 3.5 GeV. In several cases the escaping tracks showed multiple scattering which made it possible to estimate their energy. Approximately 50% of these 15 events have been retained in the sample.

From about 500 neutrino events originating inside the fiducial volume, 51 events constitute the final sample. This relative rate is in good agreement with the bubble-chamber observation (25 multiplication events with $E_{\text{visible}} > 3.5$ GeV for 245 neutrino events in the 1964 experiment). Figure 8 shows the μ^- momentum distribution for these 51 events. The muon momenta below 800 MeV/c are due mainly to events for which the muon was not recognized; the shortest non-interacting stopping track in the event has been chosen as the muon.

The expected μ^- momentum distributions³⁾ for the boson events have been drawn in Fig. 8 for $M_W = 1.5, 1.7$ and 1.9 GeV/c² with $B = 0$. These curves are computed using the Van der Meer spectrum for 29×10^{16} ejected protons and the fiducial mass of 2.3 tons. To compare the theoretical curves with the observed events, one must take into account the fact that the threshold for W production increases with the boson mass (see Fig. 3). The number of observed events with a total energy above threshold for $M_W = 1.7$ and 1.9 GeV/c² is respectively about 20% and 40% less than the number of events plotted.

It is clear from Fig. 8 that the majority of the observed events cannot be due to boson production, because the corresponding muon momenta are too high. For $B = 0$ a lower limit of about 1.6 GeV can be derived for the boson mass from the spark-chamber data.

VI. CONCLUSION

From the combined results of the spark chamber and of the bubble chamber, the lower limit for the boson mass as a function of $B = (W \rightarrow \ell + \nu/W \text{ total})$, and with a level of confidence $\geq 95\%$, can be written as:

$$M_W > (1.8 + 0.5 B) \text{ GeV/c}^2 \quad 0 \leq B \leq 1 .$$

This expression has been established under the following principal assumptions: the high-energy part of the neutrino spectrum follows the Van der Meer computations⁶⁾ and the boson production cross-sections are those given by Wu et al.⁷⁾. A change by a factor

of two either way in the product (production cross-section \times neutrino flux) would modify the limit on M_W by $\pm 0.2 \text{ GeV}/c^2$. From the low q^2 measurement⁵⁾, taking into account the uncertainty on the background, the neutrino flux above 4 GeV is estimated to be (1.5 ± 0.6) times the flux computed by Van der Meer.

Finally, in deriving the mass limit from the leptonic decays, only the "elastic" channel of W production has been considered. The cross-sections have not been computed for the "inelastic" channels, but this additional production will, in any case, increase the lower limit on the boson mass derived from the leptonic decays.

Table 1

Classification of Events

Type	Number of events
(-,? stop)	19
(+ ,? stop)	1
(?,? stop)	2
(?,+ stop)	5
(+,-)	23
(±,?)	2

Table 2

Expected and observed number of muon pairs

Boson Mass GeV	I		II		III	
	EXP	OBS	EXP	OBS	EXP	OBS
1.5	26		21		23	
1.7	16		12.5		13.6	
1.9	7.8	≤ 2	6.1	≤ 1	6.7	0
2.1	4.2		3.4		3.6	
2.5	1.1		0.9		0.95	

1. Magnetized Iron Region
- I 45 cm cuts on both tracks
 - II 55 cm cuts on both tracks
 - III 30 cm cut on negative track, and 70 cm cut on positive track.
1. Thick-plate region
- 60 cm cuts on both tracks in all three cases.

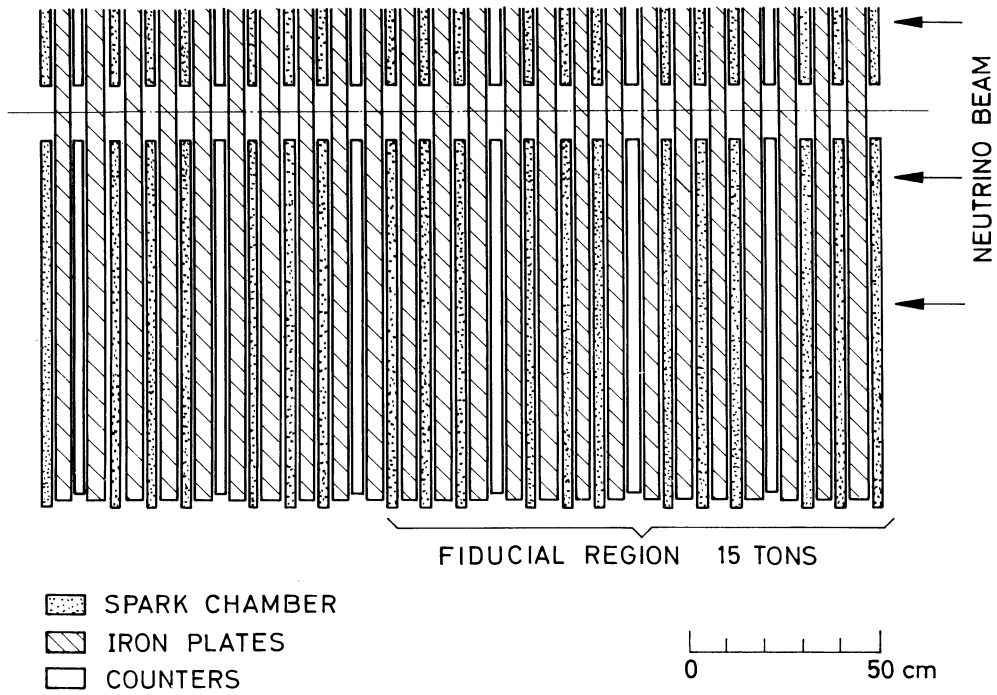
REFERENCES

- 1) J. Schwinger, *Annals of Physics* 2, 407 (1957).
B. Pontecorvo and R. Ryndin, *Proceedings of the Ninth International Conference on High-Energy Physics, Kiev (1959)*, Vol. II, p. 233.
T.D. Lee and C.N. Yang, *Phys.Rev. Letters* 4, 307 (1960).
- 2) J.S. Bell and M. Veltman, *Physics Letters* 5, 94 and 151 (1963).
- 3) M. Veltman, *Physica* 29, 161 (1963) and private communication.
- 4) M.M. Block, H. Burmeister, D.C. Cundy, B. Eiben, C. Franzinetti, J. Keren, R. Møllerud, G. Myatt, A. Orkin-Lecourtois, M. Paty, D. Perkins, C.A. Ramm, K. Schultze, H. Sletten, K. Soop, R. Stump, M. Venus and H. Yoshiki, *Physics Letters* 12, 281 (1964).
- 5) G. Bernardini, J.K. Bienlein, G. Von Dardel, H. Faissner, F. Ferrero, J.-M. Gaillard, H.J. Gerber, B. Hahn, V. Kaftanov, F. Krienen, C. Manfredotti, M. Reinharz and R.A. Salmeron, *Physics Letters* 13, 86 (1964).
- 6) S. Van der Meer, *Proceedings of the International Conference on Elementary Particles, Sienna (1963)* Vol. I, p. 536, and private communication.
- 7) A.C.T. Wu, C.P. Yang, K. Fuchel and S. Heller, *Phys.Rev. Letters* 12, 57 (1964), and private communication.
- 8) J.K. Bienlein, A. Böhn, G. Von Dardel, H. Faissner, F. Ferrero, J.-M. Gaillard, H.J. Gerber, B. Hahn, V. Kaftanov, F. Krienen, M. Reinharz, R.A. Salmeron, P.G. Seiler, A. Staude, J. Stein and H.J. Steiner, *Physics Letters* 13, 80 (1964).
- 9) M.M. Block, CERN preprint.
- 10) S.M. Berman and M. Veltman, to be published in *Nuovo Cimento*.
- 11) H.S. Mani and J.C. Nearing, *Phys.Rev.* 135B, 1009 (1964), and private communication.
- 12) CERN Heavy liquid bubble chamber group, report presented at the Informal Conference on Experimental Neutrino Physics, CERN (1965).

FIGURE CAPTIONS

- Figure 1 : Experimental set-up. Top view of the magnetized iron region.
- Figure 2 : Spectrum of the high-energy neutrinos at the spark chamber position in the CERN 1964 experiment.
- Figure 3 : Rates of boson production. The dashed portions of the curves correspond to an extrapolation of the production cross-sections.
- Figure 4 : Sagitta distribution for the stopping particles of the sample. A stopping μ^- has a 95% probability to give a point either below the top curve or above the bottom one.
- Figure 5 : Example of an event. The positive and negative tracks traverse 65 cm and 105 cm of iron, respectively.
- Figure 6 : Ranges of the positive and negative tracks for the events of the sample.
- Figure 7 : Experimental and theoretical range distributions of the positive tracks.
- Figure 8 : Experimental and theoretical distributions of the negative muon momentum.

TOTAL WEIGHT 25 TONS



MAGNETIZED IRON REGION

Fig. 1

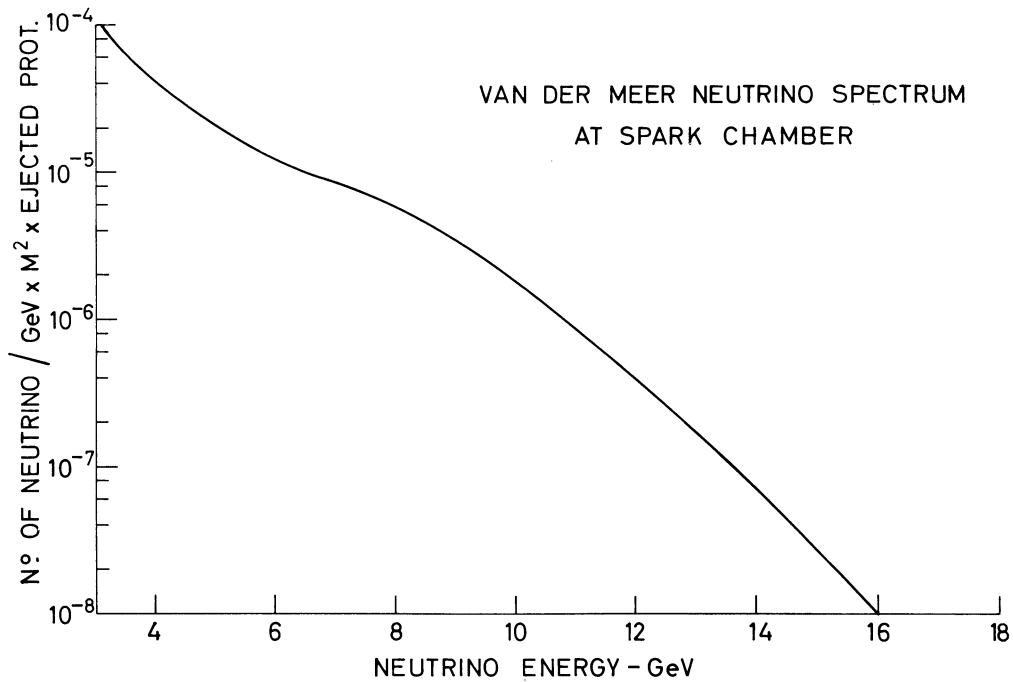


Fig. 2

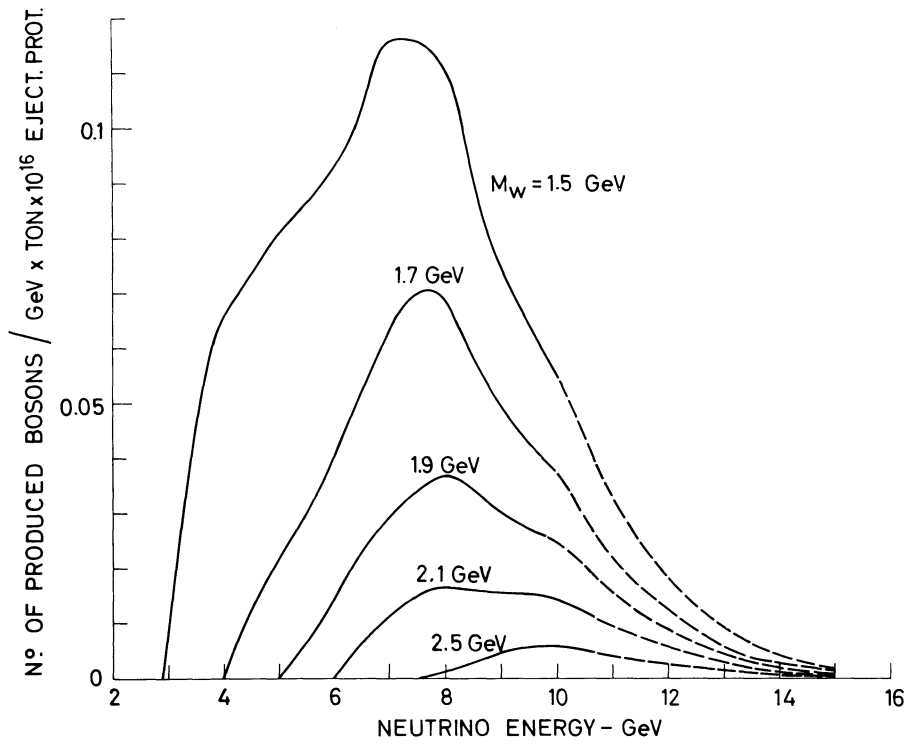


Fig. 3

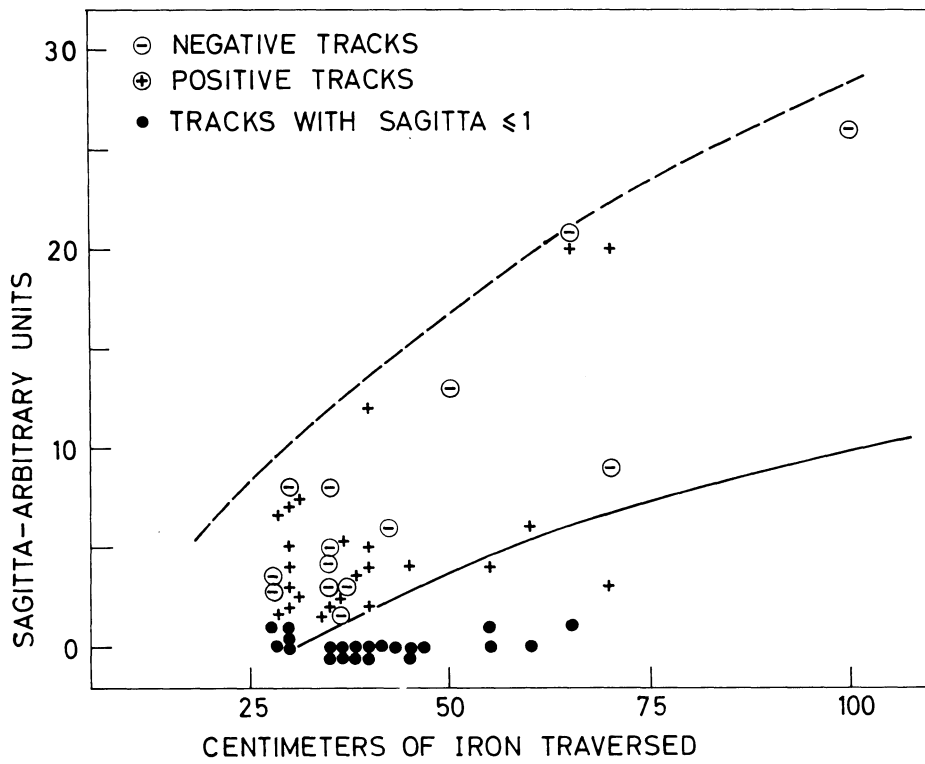


Fig. 4

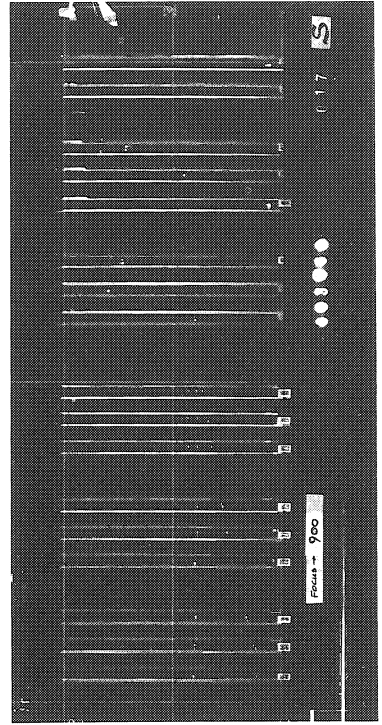
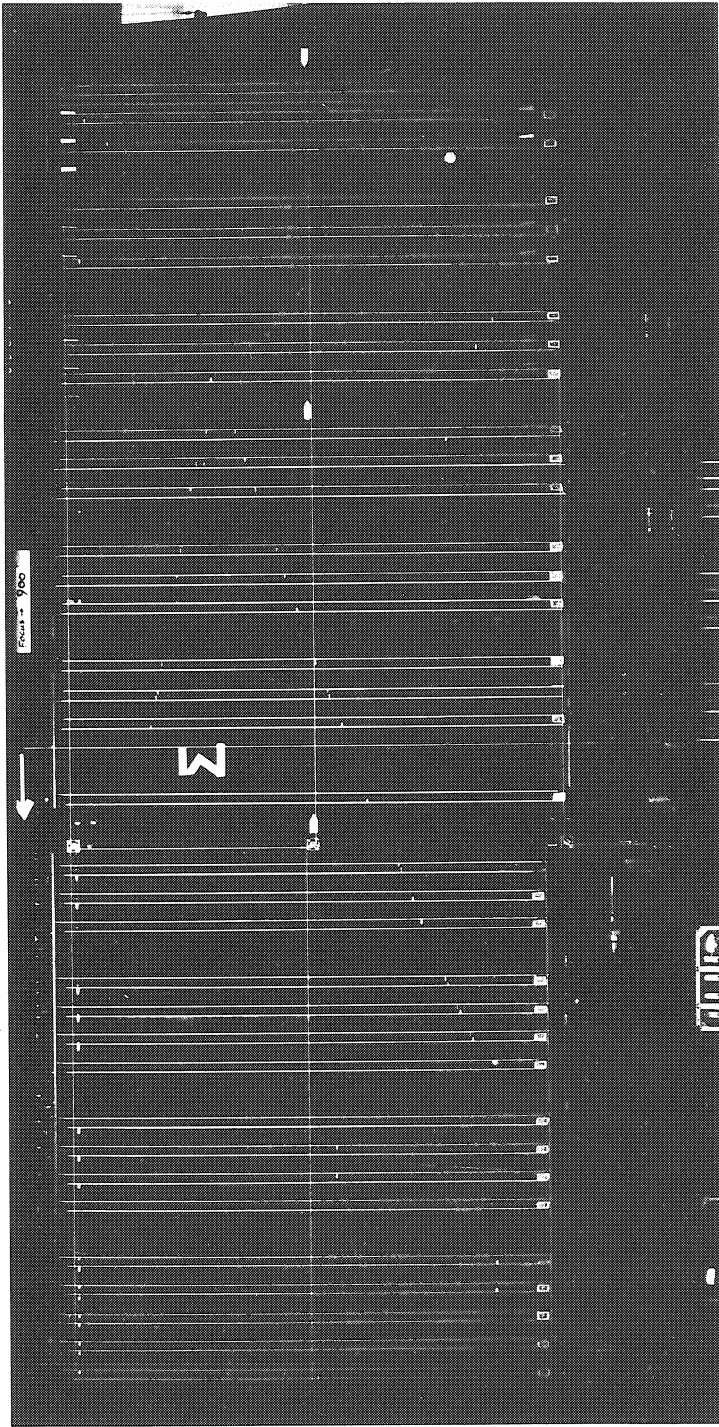


Fig. 5

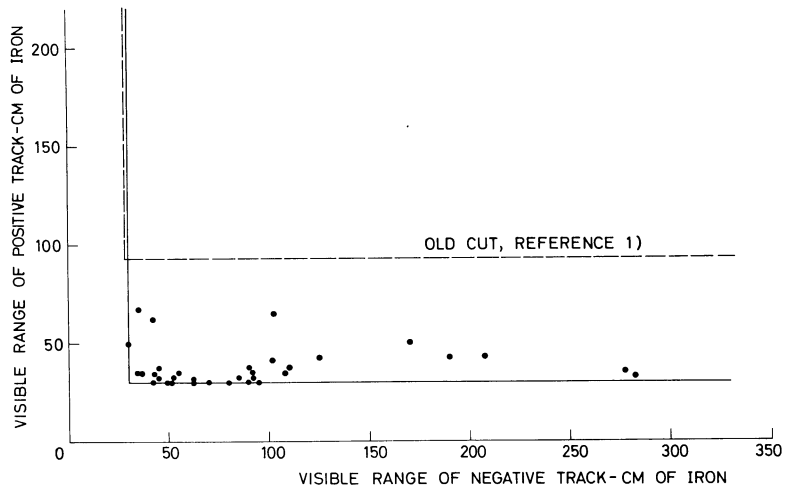


Fig. 6

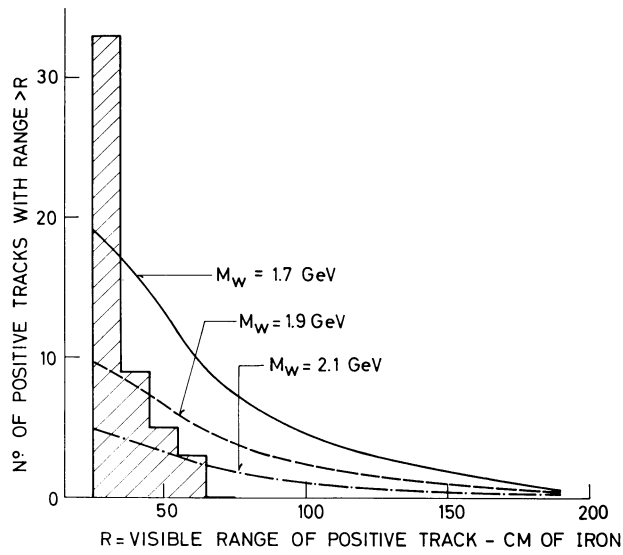


Fig. 7

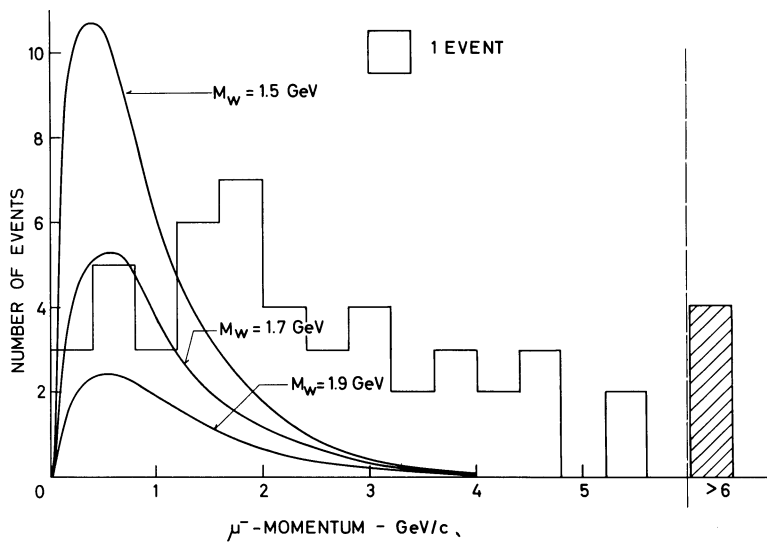


Fig. 8